Surface Science 612 (2013) 16–23

Contents lists available at SciVerse ScienceDirect

Surface Science

journal homepage: www.elsevier.com/locate/susc

# Surface effects on the structure and lithium behavior in lithiated silicon: A first principles study

Chia-Yun Chou [a], Gyeong S. Hwang [a,b,*]

[a] Materials Science and Engineering Program, University of Texas at Austin, USA
[b] Department of Chemical Engineering, University of Texas at Austin, Austin, TX 78712, USA

ARTICLE INFO

*Article history:*
Received 13 November 2012
Accepted 13 February 2013
Available online 19 February 2013

*Keywords:*
Silicon lithiation
Surface effect
Lithium mobility
Density functional theory
ab initio molecular dynamics

ABSTRACT

Silicon anodes with excellent capacity retention and rate capability have been demonstrated utilizing nanoengineered structures, such as nanowires and nanoscale thin films. Here, we present a comparative study using density functional theory calculations to examine the surface effects on the composition, structural evolution, energetics and Li-ion mobility in amorphous $Li_xSi$ alloys ($0.42 \le x \le 3.57$). When the Li content is sufficiently low, our calculations predict a slight Li surface enrichment as the presence of Li atoms contributes to the stabilization of the surfaces. As the Li content is further increased, the near-surface structure and alloy composition become similar to that in the bulk, except for the reduction in Si–Si connectivity within the outermost surface layer. The surface effects tend to be very shallow and only extend to the first couple of atomic layers; nonetheless, our ab initio molecular dynamics simulations highlight the improved Li mobility in the near-surface region. Additionally, our calculations show that Li mobility is extremely sensitive to the alloy composition, and Li diffusivity is enhanced by orders of magnitude in the highly lithiated stage.



## 1. Introduction

Silicon (Si) has recently emerged as an attractive anode material for lithium-ion (Li-ion) batteries because of its impressive energy-storage capacity. Among all the potential anode materials, Si has the highest known theoretical capacity which is one order of magnitude larger than that of graphite (the most commonly used anode material in today's Li-ion batteries) [1–5]. However, the practical use of Si as an anode material is hampered by its large volume expansion (>300%) [6–8], causing pulverization, loss of electrical contact and consequently early capacity fading. Considerable efforts have been made to overcome this drawback, including alloying Si with active/inactive elements such as tin [9,10] and transition metals [11–14], and structural modifications such as utilizing amorphous phases [15,16], nanoparticles [17,18] and nanowires (NWs) [19].

In general, Si nanostructures can accommodate larger strain and provide better mechanical integrity because their dimensions would limit the size and propagation of cracks, which typically initiate the fracture process [20–23]. Earlier studies not only highlighted the excellent capacity retention of Si NWs [19,24] and thin films [23,25], but also showed easier Li diffusion in the surface region than inside the bulk, leading to faster charge rates. Cui and co-workers [19] have reported Si NWs exhibiting 3193 mAh/g discharge capacity after 10 cycles at C/20 rate (discharge in 20 h) and stable capacity (~3500 mAh/g) up to 20 cycles at C/5 rate. Although the lengths of Si NWs increase and their volume changes appear to be about 400% after lithiation, NWs remain continuous without fractures. Similarly, Si thin films have consistently realized capacities above 2000 mAh/g; Kumta and co-workers [25] have presented amorphous 250 nm-thick Si films with reversible capacities of about 3500 mAh/g at C/2.5 rate for 30 cycles with no obvious signs of failure. While nanostructured Si exhibits many beneficial properties as an anode material, the large surface area may also cause more significant solid electrolyte interphase (SEI) formation and consequently larger capacity loss [26–29].

Recently there is an increasing number of studies employing first principles calculations to investigate lithiation of both crystalline and amorphous Si [30–33]. To study Li behavior at the onset of lithiation, researchers also looked at single Li insertion into Si NWs with different axis orientations and sizes [34,35]. It was shown that surface sites are energetically the most favorable insertion positions, and the diffusion barrier is smaller compared to that in the bulk; in other words, an accelerated Li diffusion can be promoted by shrinking the size of the nanocrystal. However, as the Li content increases, it is practical to look at the alloy formation and Li behavior in amorphous silicon–lithium alloys (*a*-Li–Si) as they are commonly observed during room-temperature lithiation (solid state amorphization) [36]. To the best of our knowledge, there have not been atomistic level studies to specifically address the alloying and structural properties of lithiated Si (*a*-Li–Si) in the near-surface region.

In this work, we use density functional theory (DFT)-based ab initio molecular dynamics (AIMD) to determine the near-surface structures for *a*-$Li_xSi$ alloys of various Li contents ($0.42 \le x \le 3.57$). The structural

* Corresponding author at: Department of Chemical Engineering, University of Texas at Austin, Austin, Texas 78712, USA. Tel./fax: +1 512 471 7060.
*E-mail address:* gshwang@che.utexas.edu (G.S. Hwang).

0039-6028/$ – see front matter © 2013 Elsevier B.V. All rights reserved.
http://dx.doi.org/10.1016/j.susc.2013.02.004

evolution and energetics in the near-surface region of the alloys are compared with those in the bulk. In particular, we discuss the surface atomic composition and Si–Si coordination along the direction perpendicular to the surface to demonstrate the surface effects on the structure arrangement and incorporation of Li. In addition, AIMD simulations are performed to access the surface effects on the mobility of Li atoms in *a*-Li–Si alloys. The fundamental findings from this theoretical work should provide some insight into the surface effects on the lithiation and delithiation processes of nanostructured Si, while complementing existing experimental observations and also contributing to a better understanding of the lithiation mechanism of Si-based nanomaterials.

## 2. Computational methods

Quantum mechanical calculations reported herein were performed on the basis of DFT within the generalized gradient approximation (GGA-PW91) [37], as implemented in the Vienna Ab-initio Simulation Package (VASP) [38–40]. Spin polarization of the Li–Si system was also examined, but appears to be insignificant. The projector augmented wave (PAW) method with a planewave basis set was employed to describe the interaction between ion cores and valence electrons. The PAW method is, in principle, an all-electron frozen-core approach that considers exact valence wave functions. Valence configurations employed are: $1s^2 2s^1$ for Li and $3s^2 3p^2$ for Si. An energy cutoff of 350 eV was applied for the planewave expansion of the electronic eigenfunctions. During geometry optimization, all atoms were fully relaxed using the conjugate gradient method until residual forces on constituent atoms become smaller than $5\times10^{-2}$ eV/Å.

The model structures for bulk *a*-Li–Si alloys were created using AIMD simulations (see Refs. [41] and [42] for detailed computational methods). The *a*-Li–Si structures considered are summarized in Table 1; three different supercells were constructed for each alloy composition. The initial slab models were prepared by introducing a 15-Å-thick vacuum gap into the *a*-Li–Si bulk alloys in the *z* direction (for each alloy composition, three different slab models were prepared based on their corresponding bulk structures). To simulate a laterally extended surface in the *x* and *y* directions, we employed the repeated-slab approach by applying periodic boundary conditions to the unit cell in all dimensions as illustrated in Fig. 1. The thinner slab (slab A) contains 64 atoms while the thicker slab (slab B) containing 128 atoms was prepared by stacking two identical 64-atom bulk models in the *z* direction. The slab models were then annealed at 800 K for 4 ps and 300 K for 1 ps to allow sufficient atomic redistribution and relaxation, followed by static energy minimization of the alloy structures. For Brillouin zone sampling, a $(2\times2\times2)$ *k*-point mesh in the scheme of Monkhorst–Pack [43] was used for all bulk amorphous samples summarized in Table 1, and for the corresponding slab models, a $(2\times2\times1)$ *k*-point mesh was used. We carefully checked the convergence of atomic configurations and relative energies with respect to calculation conditions including planewave cutoff energy and *k*-point mesh size.

**Table 1**
Compositions and optimized supercell volumes of the *a*-$Li_xSi$ alloys examined in this work.

| *x* in *a*-$Li_xSi$ | #Li/#Si | Volume (Å$^3$/Si) |
|---|---|---|
| 0.42 | 19/45 | 24.5 |
| 1.00 | 32/32 | 32.9 |
| 1.29 | 36/28 | 37.8 |
| 1.67 | 40/24 | 43.3 |
| 2.05 | 43/21 | 49.6 |
| 2.56 | 46/18 | 58.2 |
| 3.00 | 48/16 | 65.2 |
| 3.57 | 50/14 | 74.8 |

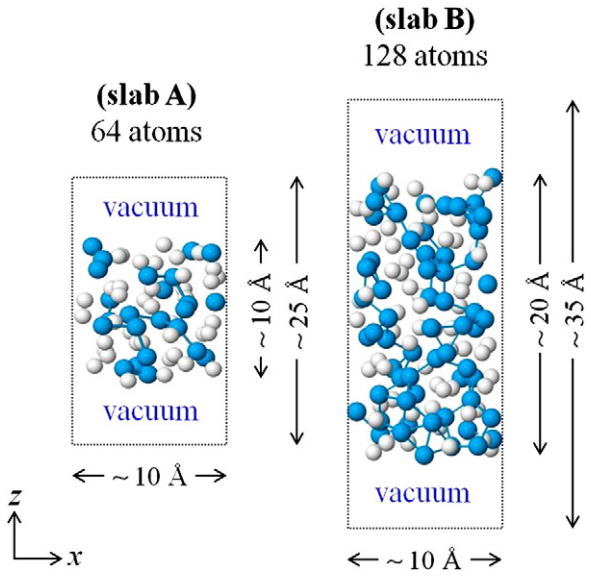


**Fig. 1.** Side view of *a*-Li–Si slab systems containing 64 atoms (slab A) and 128 atoms (slab B); *x* and *y* dimensions are approximately equal. The white and blue (dark grey) balls represent Li and Si atoms, respectively. The laterally extended surface in the *x* and *y* directions is simulated using the repeated slab approach with a vacuum layer inserted in the *z* direction.

## 3. Results and discussion

### 3.1. Surface effect on alloy composition and structure

#### 3.1.1. Surface composition

We examined the variations in Li concentration within the outermost layers of slabs A and B, in comparison with the corresponding bulk counterparts. In Fig. 2, the dashed line with unit slope marks the surface Li concentration being identical to that in the bulk. Here, as also illustrated in Fig. 2 (left panel), we chose the outermost surface layer to be composed of atoms whose surface-projected coordinates have no overlap with other atoms near the surface [44]; the

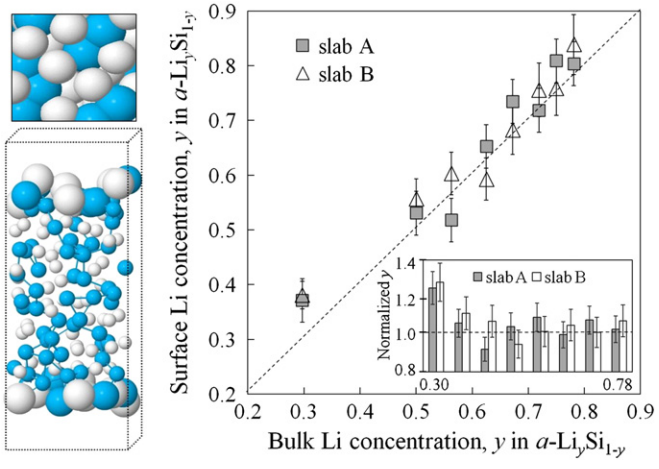


**Fig. 2.** Comparison between the surface and bulk Li concentrations (*y* in *a*-$Li_ySi_{1-y}$). The surface composition was obtained by averaging over the top and bottom surfaces (as illustrated in the left panel) of three independent slabs. The white and blue (dark grey) balls represent Li and Si atoms respectively, and the surface atoms are larger in size than that in the bulk. The dash line of slope = 1 marks the surface Li concentration being identical to that in the bulk. The inset shows the normalized surface Li concentrations (with respect to the corresponding bulk values).